hapter for the Toulouse volume, Solar System Ices

es on the Satellites of Jupiter, Saturn, and Uranus

Dale P. Cruikshank
NASA Ames Research Center, MS 245-6
Moffett Field, CA 94035-1000, USA
e-mail: cruikshank@ssa1.arc.nasa.gov
Phone: 415-604-4244, FAX 415-604-6779

Robert H. Brown
Jet Propulsion Laboratory, MS 183-501
4800 Oak Grove Dr.
Pasadena, CA 91109, USA

Wendy M. Calvin
U.S. Geological Survey, Branch of Astrogeology
2255 North Gemini Dr.
Flagstaff, AZ 86001, USA

Ted L. Roush
San Francisco State Univ. and NASA Ames Research Center
Moffett Field, CA 94035-1000, USA

ABSTRACT

Three satellites of Jupiter, seven satellites of Saturn, and five satellites of Uranus show spectroscopic evidence of H_2O ice on their surfaces, although other details of their surfaces are highly diverse. The icy surfaces contain contaminants of unknown composition in varying degrees of concentration, resulting in coloration and large differences in albedo. In addition to H_2O, Europa has frozen SO_2, and Ganymede has O_2 in the surface; in both of these cases external causes are implicated in the deposition or formation of these trace components. Variations in ice exposure across the surfaces of the satellites are measured

from the spectroscopic signatures. While H_2O ice occurs on the surfaces of many satellites, the range of bulk densities of these bodies shows that its contribution to their overall compositions is highly variable from one object to another.

1. Introduction

One of the early important results of the application of near-infrared detectors on large telescopes to Solar System problems was the discovery of absorptions due to H_2O ice on Europa and Ganymede (Kuiper 1957). The history of this and subsequent discoveries has been reviewed several times (e.g., Sill and Clark 1982, Clark et al. 1986, Cruikshank and Brown 1986) and will not be repeated here. This chapter focuses on the current state of knowledge of the ice-covered satellites of Jupiter (excluding Io, which is discussed in Chapter *** by Nash), Saturn, and Uranus. Our current knowledge of the ices on Triton, Pluto, and Charon is reviewed in Chapter *** by Cruikshank et al. (1996).

Ices have been detected on Solar System bodies by spectroscopic observations in the near-infrared (1-2.5 μm) region of the spectrum, where the light from these bodies is sunlight diffusely reflected from their surfaces. The utility of this particular spectral region arises from several independent factors. First, the Earth's atmosphere is sufficiently transparent throughout most of this region that spectroscopy from ground-based observatories is possible. Second, the ices of simple and complex molecules have their low overtone and combination absorption bands in this spectral region, and most of these bands are sufficiently strong to allow detection at modest spectral resolution. Third, sunlight incident on the surfaces of planets and satellites is sufficiently strong in this wavelength region to yield a measurable signal. Fourth, detectors for this region have been available since about 1945, and rapid improvements in their qualities now permit spectroscopic work at high signal precision and moderate spectral resolution on bodies as distant and faint as Pluto and the larger satellites of Uranus and

Neptune (visual magnitudes 12-14).

At wavelengths longer than 2.5 μm the incident sunlight is very weak and the Earth's atmosphere is less transparent. At wavelengths shorter than 1 μm the absorption bands are higher overtones and more complex combinations, and are therefore much weaker, making detection and interpretation more difficult. There are some recent important exceptions to these general statements; O_2 in the surface ice of the trailing hemisphere of Ganymede has been found in the photovisual spectral region by Calvin and Spencer (1994, 1995) and SO_2 ice has been found by ultraviolet spectroscopy of Europa with the Hubble Space Telescope (Noll et al. 1994, 1995. Furthermore, because the four large satellites of Jupiter are quite bright, spectra of high quality have been obtained at wavelengths as long as 5 μm; the radiation from Io at this wavelength is dominated by the satellite's thermal radiation, while for Europa, Ganymede, and Callisto, diffusely reflected sunlight dominates the signal.

Detection of ices and other components on a planetary or satellite surface is an important first step in understanding the nature of that body, but the interpretation of the spectrum in a quantitative way requires additional effort that has been possible only in the last few years through the application of scattering theory. Computation of synthetic spectra of scattering surfaces, using the optical properties (real and imaginary refractive indicies) of ices measured in the laboratory, provides the capability to investigate grain size variations and mixtures of components that have not been directly measured in the laboratory. Hapke (1993a,b) has developed a series of equations describing the interaction of energy (e.g., sunlight) with particulate surfaces, and the application of his scattering theory to real planetary surfaces has proven to be very productive (e.g., Clark and Roush 1984, Clark and Lucey 1984, Calvin et al. 1995a, Wilson et al. 1994, Wilson and Sagan 1995, Roush et al. 1990, Owen et al. 1993, Cruikshank et al. 1993, Roush 1994).

The general equation describing the bidirectional reflectance of a surface is

$$r(i,e,g,\bar{w},h,S(0),b,c,\bar{\Theta}) = \frac{\bar{w}}{4\pi}\frac{\mu_o}{\mu_o+\mu}\{[1 + B(g)]P(g) + H(\mu_o)H(\mu) - 1\},$$

where i and e (μ_o = cos i, μ = cos e) are the angles of incident and emergent light, g is the phase angle between i and e, and w is the average single scattering albedo of the surface. Compositional information is contained in the parameter w that is related to the absorption coefficients of individual components in a mixure. From the measured real and imaginary indices of potential materials (ices, minerals, organic solids, etc.), the reflectance can be calculated via equation 1 and directly compared to the observational data. Roush's development of the Hapke scattering theory and its application to icy surfaces is given in Roush et al. (1995) and in the Appendix in Chapter *** by Cruikshank et al. (1996).

An example of such calculations for various grain sizes of H_2O ice (at a temperature near the freezing point) is illustrated in Figure 1.

2. The Galilean Satellites of Jupiter

Although the icy polar caps of Mars had been observed for several decades, the discovery of solid H_2O absorptions on Europa and Ganymede represented the first detection by near-infrared spectroscopy of ice on any other solar system body. Improvements in detector technology have made it possible to study the H_2O bands in considerable detail, as well as on Callisto, where the bands are significantly weaker than on Europa and Ganymede.

The large satellites of Jupiter are not globally homogeneous in their physical properties as was first evident from the observation that their brightnesses vary as they revolve about Jupiter in their orbits. Spectroscopic observations show that

the strength and character of the ice absorption bands is also variable on a global scale, and the images of the satellite surfaces from Voyagers 1 and 2 adequately demonstrate not only the vast differences from one satellite to another, but significant differences around the globe of any single satellite. In the present context we describe the global variation of the near-infrared reflectance, using the terms "leading" and "trailing", where "leading" refers to the hemisphere facing the direction of the satellite's orbital motion.

We consider each of Europa, Ganymede, and Callisto in turn, following the recent review by Calvin et al. (1995a), which should be consulted for more details on various sources for specific parts of each spectrum and for the criteria on which basis the composite spectra were assembled.

2.1 Europa

The spectra of the leading and trailing hemispheres of Europa are shown in Figure 2, which was compiled by Calvin et al. (1995a) from several sources, as listed in Table II. The large difference in the geometric albedos at various wavelengths between the leading and trailing hemispheres is evident. A comparison of the leading hemisphere spectrum with a scattering model using 100 μm H_2O ice shows the coincidence of the band positions and a general agreement in the overall shape of the spectra (1-2.5 μm), but distinct differences (Figure 3). The divergence of the spectra indicates that while H_2O is the principal constituent of the surface, a single particle size is probably not a suitable model for that ice, and other material must also occur there.

The strong absorption on Europa at wavelengths <0.5 μm is a signature of the non-H_2O component(s). Spencer et al. (1995) propose that the departure from the high reflectance of H_2O toward the ultraviolet is consistent with the presence of sulfur-bearing species and possibly allotropes of pure S. A

broad UV absorption feature was first noticed on Europa by Lane et al. (1981), who suggested implanted S ions in the H_2O ice on the surface. Ockert et al. (1987) mapped the variable strength of this band around Europa, showing that it is strongest on the trailing hemisphere. Noll et al. (1995) used the Hubble Space Telescope to detect a discrete absorption band centered at 2800 A (full width ~600 A) on Europa, and found that it is best matched by a thin layer of SO_2 ice grown on H_2O, using laboratory data by Sack et al. (1992). Several options exist for the source of the SO_2 (Noll et al. 1995).

Recent observations in the ultraviolet (<0.4 μm) suggest that spectral changes occur on timescales of a few years. Domingue et al. (1994) have presented preliminary evidence for changes on Europa since the observations by Nelson et al. (1987a) with the International Ultraviolet Observer satellite, and further details are awaited.

Brown et al. (1988) sought to identify absorptions seen in some spectra of Europa's trailing hemisphere at 1.8 and near 2.2 μm with the ammonium ion, specifically in ammonia hydrate. Subsequent observations have failed to confirm the presence of the absorption features (Calvin et al. 1995; Cruikshank et al. unpublished). While the bands may have been transient features in the spectrum, a more plausible explanation is that they resulted from systemmatic errors in data reduction, as described by Calvin et al. (1995a).

Between 2.8 and 4.1μm, both leading and trailing hemispheres of Europa have very low reflectance; the spectrum of the trailing side shows a nearly flat spectral reflectance with geometric albedo between 0.01 and 0.02. Lebofsky and Feierberg (1985) suggest that the low albedo and absence of a reflectance peak at 3.5 μm indicates an absence of small ice particles and possible other effects caused by intense bombardment by Jupiter's magnetospheric particles. The leading hemisphere has a slightly higher reflectance (0.025 at 3.6 μm), with a broad peak from 3.5

to 3.7 μm. No evidence has yet been found for SO_2 absorptions in this region of Europa's spectrum, though they might be expected in view of the discovery of the ultraviolet SO_2 band, as noted above. The SO_2 spectrum is best shown in recent data by Schmitt et al. (1994).

The spectroscopic evidence for ice grains of particular sizes is supplemented by measurements of the photometric scattering properties of Europa. While this is a departure from the main focus of this chapter, we note that Dominque et al. (1991) deduce a surface relief at cm scales much lower than other solar system bodies. If the small opposition surge at small phase angles observed for Europa is due to particle shadowing, the implied high porosity (~96%) is greater than would be expected for micrometeorite gardening, and may be further evidence for magnetospheric surface modification. At the same time, Buratti (1991) cite photometric evidence for a less compacted trailing hemisphere than leading, again evidence for surface alteration by the magnetospheric particle flux sweeping past the satellite from its backside.

2.2 Ganymede

The spectral reflectance of Ganymede has been measured from 0.24-5.2 μm. Calvin et al. (1995a) compiled the relevant data to produce the composite spectra of the leading and trailing hemispheres shown in Figure 4. The band shapes and depths are consistent with H_2O ice on Ganymede with grain sizes of a few hundred micrometers to 1 mm. The overall shapes of the spectra of Europa and Ganymede are different; the lower albedo of Ganymede around 1 μm suggests that there is more non-ice contamination on Ganymede than on Europa, while Ganymede's albedo beyond 3 μm is significantly higher than Europa's. These differences probably result from the separate effects of the abundance and nature of the non-ice contaminants and the space weathering influence of the magnetospheric environment that affects Europa more than Ganymede.

At wavelengths longer than 2.5 μm, the spectrum of Ganymede has not been fully explored, although Calvin et al. (1995a) have detected spectral structure attributable to a non-H_2O ice component as yet unidentified.

The depths of the ice bands on Ganymede's trailing hemisphere suggest H_2O of high purity (90 weight percent) and in larger grains than on the leading hemisphere (Clark et al. 1986). Other differences may arise from the presence of additional absorbers on the trailing hemisphere. For example, the trailing hemisphere of Ganymede shows two narrow absorption bands at 0.577 and 0.675 μm that Spencer et al. (1995) have identified as condensed O_2 in the H_2O ice. This molecular oxygen is probably produced in the H_2O ice by magnetospheric plasma bombardment (Calvin et al. 1995b)

Buratti (1991) used full disk images of Ganymede (and Callisto) from Voyager I and II, plus ground-based telescopic observations, to establish the complete solar phase curves of the satellites' leading and trailing hemispheres. From such information and disk-resolved measurements from Voyager she derived the parameters required for scattering model calculations in which the the single particle phase function, the compaction state of the optical surface, and the mean slope angle of macroscopically rough surface features were all found. Buratti's analysis showed Ganymede to be uniform in all these properties, while Callisto's leading hemisphere consists of particles that are more strongly backscattering and less compacted than on the trailing hemisphere.

2.3 Callisto

Spectra of Callisto from the compilation by Calvin et al. (1995a) are shown in Figure 5. Any leading-trailing hemispheric spectral and albedo asymmetry is very small; in the spectra in Figure 5 the trailing hemisphere is only slightly brighter than the

leading. Several H_2O ice absorptions appear, including the 1.04- and 1.25-μm bands that indicate large (mm to cm size) grains, but the overall shape of the spectra show that ice is not the dominant surface constituent. The leading hemisphere has in addition to the large grain structure, a component of smaller grains (~50 to a few hundred micrometers) of H_2O ice, as evidenced by the spectral profile in the 3-3.6 μm spectral region (Calvin and Clark 1993).

Spectra of Callisto obtained between 1978 and 1985 with the International Ultraviolet Explorer satellite (Nelson et al. 1987a) have recently been reprocessed by Lane et al. (1994), and show spectral features between 0.250 and 0.320 μm, in addition to a possible broad absorption band between 0.240-0.330 μm on the trailing hemisphere. The SO_2 band reported by Noll et al. (1995) on the trailing hemisphere of Europa has a very similar wavelength extent to that noted by Lane on Callisto.

Efforts to identify the non-ice components have been focused on the region longer than 2.5 μm, notably in the work by Roush et al. (1990) and Calvin and Clark (1991, 1993). Roush et al. (1990) modeled the spectrum with three components; ice, magnetite, and serpentine, in homogeneous (intimate) and heterogeneous (areal) mixtures [see Appendix in Cruikshank et al., Chapter *** this volume]. Magnetite is a rock-forming iron oxide mineral, and serpentine (a phyllosilicate) is a hydrothermal alteration product of olivine and pyroxene, which are the primary silicate minerals that form in equilibrium condensation scenarios of Solar System formation. Roush et al. found that the three-component intimate mixtures best fit the spectrum of Callisto, and show that H_2O ice contributes more to the spectrum of the leading hemisphere than the trailing hemisphere of the satellite (Figure 6). Calvin and Clark (1991, 1993) propose phyllosilicate minerals, including ammoniated clays, as candidates for the non-ice component on Callisto; phyllosilicate minerals are found as aqueous alteration products of silicate minerals in some carbonaceous meteorites. Such

alteration products may form on icy bodies as a consequence of local impact melting of the surface ices.

2.4 Galilean Satellites--Summary

The three large satellites of Jupiter showing spectral evidence for H_2O ice are quite diverse, both in terms of the spectral signatures and their global variations, and in terms of their surface structures seen in the high-resolution pictures from the Voyager spacecraft. The differences in bulk densities of these satellites and the progression to lower density at larger distance from Jupiter are in interesting conrast to the apparent amount of H_2O ice on their surfaces: Europa, the most dense, appears to have less water in its interior and more on the surface, while much lower density Callisto retains water in the interior and has less exposed on the surface.

The structures of the surfaces ices of the Galilean satellites are influenced by the flux of impacting micrometeoroids and the flux of atomic particles trapped in Jupiter's magnetosphere and sweeping by the satellites as the magnetosphere rotates. The microphysical and chemical influences of the magnetosphere and micrometeorid fluxes continue to be topics of great interest among researchers.

The Galileo mission to Jupiter will focus intense interest on the large satellites, providing compositional maps of high spatial resolution of much of their surfaces. We can expect important new information and understanding of the nature of the surfaces of these bodies where H_2O ice was first discovered by telescopic observers.

2.5 Small Satellites of Jupiter

Twelve small satellites of Jupiter are known, but there is no direct evidence that their surfaces are icy. Their generally low albedos suggest that ice is not present (Thomas et al. 1986).

3. The Icy Satellites of Saturn

Spectroscopic observations have shown the clear presence of H_2O ice on the surfaces of seven satellites and the rings of Saturn (Table I), and ice may be a component of the surfaces of at least some of the satellites that are too faint or too close to the planet to be observed from Earth (Morrison et al. 1984; Cruikshank et al. 1986; Thomas et al. 1986). The low mean densities of the satellites confirm that H_2O is a principal component of their interior compositions as well.

Clark et al. (1984) presented a series of spectra of the leading and trailing hemispheres of Rhea, Dione, Tethys, and Iapetus (0.65-2.5 μm) demonstrating differences in H_2O band strengths and shapes related to the albedos and the ice particle scattering properties on the satellite surfaces. The spectrum of one hemisphere (leading) of Enceladus was included in their study. The leading hemisphere of Iapetus is a special case discussed below. The data for some of the satellites have sufficient signal precision to show the 1.04-μm band that is particularly diagnostic of mean optical path within the surface layer of H_2O ice. On Rhea, the depth of this band corresponds to a 1 mm mean optical path length in H_2O ice, suggestive of a surface relatively free of opaque contaminants. The ice appears to be of similar purity on Tethys, Dione, and the trailing hemisphere of Iapetus, although the ice bands are typically stronger on the leading hemispheres than they are on the trailing hemispheres.

Clark et al. (1984) suggested that the leading-trailing asymmetry seen on some satellites is related to magnetospheric interaction, as appears to be the case for the Galilean satellites of Jupiter. Chapter *** of this book reviews current thinking on this important subject.

3.1 Mimas

There is no direct spectral evidence for ice on Mimas, but its high geometric albedo at 0.55 μm (p_V=0.8; Buratti et al. 1990a) suggests that material of high reflectivity, such as pure H_2O ice, occurs there. Variations of the brightness of Mimas in the Voyager images at wavelength 0.48 μm are <10%, with the lealding side possibly a few percent brighter than the trailing side (Buratti et al. 1990a).

3.2 Enceladus

The small angular separation of Enceladus from Saturn's rings has made spectral observations from Earth difficult, but there is clear evidence for H_2O ice (Cruikshank 1980, Clark et al. 1983). Enceladus has the highest geometric albedo of any known airless body in the Solar System, p_V=1.0 (Buratti et al. 1990a). The high albedo and flat spectrum between 0.35 and 0.59 μm demonstrate that the surface ice has less included opaque materials than the other Saturn satellites have. Leading-trailing hemispheric differences in color and albedo are very small.

3.3 Tethys

The evidence for H_2O ice is clear on Tethys, as shown in Figure 7. The leading-trailing asymmetry is also pronounced, with the leading hemisphere some 10-15% brighter (p_V=0.8) than the trailing; the trailing side is also slightly redder than the leading side in the Voyager photometry (Buratti et al. 1990a).

3.4 Dione

The H_2O ice bands are very strong on Dione (Figure 7), although the geometric albedo of this satellite is the lowest of the large, icy satellites of Saturn. For the leading hemisphere, p_V=0.55, and the trailing hemisphere is about 0.4; details of the distribution of albedo and color (from Voyager images) are given

by Buratti et al. (1990a).

3.5 Rhea

Prominent H_2O ice bands occur over Rhea's entire surface; the leading hemisphere (p_V=0.65) is about 20% brighter than the trailing hemisphere (Buratti et al. 1990a; Verbiscer and Veverka 1989). Recent searches for NH_3 and CO_2 in Rhea's surface ices have not yielded detections (Griffith et al. 1995), although NH_3 in particular is a plausible component that may be related to relatively recent resurfacing events on the satellite. (e.g., Stevenson 1982).

3.6 Hyperion

The strengths of the H_2O ice bands on Hyperion are similar to those of Ariel (see below), as Brown (1983) noted before the geometric albedo for Ariel was measured. For Hyperion p_V=0.25 and for Ariel p_V=0.31 (Buratti et al. 1990b). Hyperion is an unusual satellite of irregular shape and chaotic rotation, suggestive of a relatively recent disruptive impact. The spectral geometric albedo in the range 0.3-1.0 μm decreases toward shorter wavelengths more sharply than the other Saturnian satellites (except Iapetus' dark hemisphere), suggesting the presence of a red-colored contaminant in the surface ice, or perhaps a partial covering of the surface from an external source (cf. Thomas and Veverka 1985 for this and a review of all the Voyager observations).

3.7 Iapetus (Trailing Hemisphere)

Strong H_2O ice bands and p_V=0.5 characterize this surface (Clark et al. 1984), which is spectrally similar to Dione, Tethys, and Rhea.

3.8 Iapetus (Leading Hemisphere)

The leading hemisphere of Iapetus is covered with a very low-albedo (p_V=0.04), red coating of material of uncertain composition, probably from an external source (e.g. Bell et al. 1985, Buratti and Mosher 1995). The dark red material is probably a complex organic solid (c.f. Bell et al. 1985, Wilson and Sagan 1995). H_2O ice is seen in the extreme polar regions of the leading hemisphere because of the peculiar way in which the dark material is deposited.

3.9 Small Satellites of Saturn

The small, irregularly shaped satellites of Saturn have geometric albedos in the range 0.5-0.9, suggestive of icy surfaces, although no infrared spectra have been obtained. Thomas et al. (1986) reviewed our understanding of these small bodies.

3.10 Summary, Saturn's Satellites

The seven large satellites of Saturn (excluding Titan) are a diverse collection of bodies with geological structures showing evidence of impacts, tectonic modification of their crusts, partial or complete resurfacing by endogenic and exogenic activity, and more (Morrison et al. 1984, 1986). The presence of H_2O ice on their surfaces unifies them in the context of this chapter. Only H_2O ice has been identified, but a thorough study of the infrared spectra of high quality may reveal additional surface components.

4. The Icy Satellites of Uranus

The five largest satellites of Uranus (Table I) show the signature of H_2O ice in their reflectance spectra, as seen in Figure 8. Cruikshank (1980) found the H_2O ice bands in spectra of Titania and Oberon, while a later study by Cruikshank and Brown (1981) revealed these bands on Titania and Oberon. The evidence for ice is weakest for Miranda because this satellite is very faint as seen from Earth, and adequate spectroscopic data

are very difficult to obtain (Brown and Clark 1984). Soifer et al. (1981) published spectrophotometry of Umbriel, Titania and Oberon which confirmed the discovery of H_2O ice absorptions and for the first time raised the possibility that these bodies are somewhat lower in albedo than other icy planetary satellites. Thermal emission measurements of the satellites by Brown et al. (1982) confirmed the low albedos and permitted the first reliable determinations of the satellite diameters. The diameters and albedos now used are those derived from the Voyager 2 flyby in 1986 (Buratti et al. 1990b).

Although Miranda has a higher albedo than the other four, the spectral geometric albedos of the remaining four large satellites are somewhat lower than those of the satellites of Saturn, and are more similar to Ganymede and Callisto; this fact suggests that the surface ices are contaminated to varying degrees by non-ice materials of low albedo. Spectrophotometry of Titania and Oberon (0.3-1.0 μm) by Bell et al. (1979) showed that these two satellites are remarkably neutral in color; composite spectra of these two satellites were published by Brown (1982) and in the review by Cruikshank and Brown (1986).

Measurements with the Voyager photopolarimeter (PPS) and the images taken with different filters (ISS) confirmed the low spectral geometric albedos and neutral colors of the five large satellites in the wavelength range 0.25-0.76 μm (Nelson et al. 1987b). In a more recent analysis of the Voyager color imaging data for the Uranian satellites, Buratti et al. (1990b) made small adjustments to the values of the geometric albedo, noting small differences with the earlier results of Nelson et al. and other investigators. The study by Buratti et al. combines all of the available Voyager and ground-based observational data to derive the full range of photometric properties: spectral geometric and Bond albedos, phase integrals, the color-dependent phase coefficient, and the integrated solar phase curves. These parameters are essential to characterization of the surface microstructures and the complete modeling of the surface

reflectance. Such models of the spectral reflectance have not yet been accomplished; reference should be made to the Buratti et al. (1990b) paper for their results on the microstructure, compaction, particle phase functions, etc.

Early spectral models by Brown (1983) showed that areal mixtures of H_2O frost and isolated patches of dark, neutral material (e.g., charcoal) provide approximate (but not unique) matches to the near-infrared spectra (1-2.5 μm) of Titania, Umbriel, Ariel, and Oberon. More rigorous models can now be calculated with the improved spectral geometric albedo information on each satellite, the wider wavelength range of spectral coverage, and improved modeling techniques (e.g., Roush 1994, Roush et al. 1990, 1995; Calvin and Clark 1991, 1993, Wilson et al. 1994, Wilson and Sagan 1995).

As noted by other investigators (e.g., Nelson et al. 1987b; Veverka et al. 1987), the five large satellites of Uranus comprise a unique class of bodies having low spectral geometric albedo and neutral colors in the visual spectral region, but there are significant differences among them in terms of their surface physical properties. Buratti et al. (1990b) point out that Ariel, Titania, and Oberon have very porous regoliths in which less than 10% of the volume is occupied by matter (similar to Callisto and Io), whereas Umbriel's surface is significantly more compact (similar to Ganymede).

The nature and origin of the neutral dark material contaminating the surface ices of the Uranian satellites has not been established with confidence. In a study of Voyager images of Miranda, Hillier et al. (1989) noted that the grey color of this satellite is consistent with a mixture of water ice and material similar to that covering the F-type asteroids. Spectroscopic searches for trace constituents of ices other than H_2O have not yielded any reliable detections (Brown and Cruikshank, work in progress), the spectral neutrality of the material is itself a deterrent to identification. Plausible candidates include

carbon-rich, macromolecular organic solids of the kind found in carbonacous meteorites. Thompson et al. (1987) showed experimentally that H_2O ice with enclathrated CH_4 will quickly become colored (red) and then darken to a neutral, low-albedo complex substance as energy is deposited in the form of irradiation by charged particles. Similarly, Lanzerotti et al. (1987) demonstrated that the ion and electron fluxes measured by Voyager's LECP experiment in the Uranian magnetosphere are sufficient to darken ices containing mixtures of simple organic molecules on very short timescales of a few thousand years.

The environment of the circum-Uranian space occupied by the satellites and the rings is a complex one in which dust is accreted from external sources (e.g., comminuted bodies in the Kuiper belt), debris is produced locally by bodies impacting on all of the satellites, and the flux of charged particles in the Uranian magnetosphere intercepts each of the satellites to a varying degree. In such an environment it is not difficult to envision qualitatively the effects we observe in our spectrophotometry of these satellites, even if we cannot yet establish rigorously just which effects dominate the physical processes that operated in the past and continue in the present.

4.1 Small Satellites of Uranus

Uranus has ten known small satellites, all discovered by Voyager. There is no direct evidence for ice on any of them; their measured and inferred low albedos are low, suggesting that ices do not dominate their surfaces (Veverka et al. 1991).

5. General Summary

While the largest satellites of three planets show the spectral signature of H_2O ice, these 15 objects are highly diverse in terms of their bulk properties (dimensions, densities), photometric properties and geologic surface structures. Furthermore, their histories of surface modification by impact,

melting, tectonism and other forces differ greatly from one to another. While they share the basic compositional similarity of water ice on their surfaces, even their spectral reflectances differ greatly from one to another. We demonstrate this with Figure 9, which shows an icy satellite from Jupiter, Saturn, and Uranus, each of which has the characteristic H_2O ice absorption bands. These satellites differ in terms of contamination of the surface ices (judged from the albedo levels), single-scattering albedo of the surface particles, and basic "color" in the visible region of the spectrum. The continued exploration of the spectra of these bodies in search of the reasons and deeper implications of these differences should be a matter of high priority for planetary scientists.

The principal achievements in the study of the icy satellites of Jupiter, Saturn, and Uranus since the first conference on Ices in the Solar System (Nice, 16-19 January 1984) include: (1) further analysis of Voyager data for the satellites of Jupiter and Saturn (2) the Voyager encounter with the Uranus system was accomplished in 1986; (3) new ices have been found on Europa and Ganymede with Earth-based telescopes and the Hubble Space Telescope; and (4) important new modeling tools have been developed for the computation of synthetic spectra to match the infrared data for icy satellites.

Important work remaining to be done includes: (1) obtaining better spectra (higher signal precision and higher spectral resolution) of the satellites of Saturn and Uranus with Earth-based telescopes, and applying new computational models (with a grain-size distribution and additional components) to those spectra, (2) search for additional volatile and refractory components, especially NH_3 and carbon-bearing molecules, in the spectra of all the satellites, and (3) conduct laboratory studies of space weathering and solid-state photolytic and radiation chemistry.

This chapter was written on the eve of the orbiting of the

Galileo spacecraft around Jupiter. Broad and detailed improvements of our understanding of the icy satellites of Jupiter are expected to ensue as the four-year epoch of Galileo encounters with the satellites unfolds.

6. Acknowledgments

This research is supported by NASA Planetary Astronomy RTOP 196-41-67-03 (Cruikshank), NASA Planetary Geology and Geophysics RTOP 151-01-60-01 (Roush), and ***

TABLE I Ices on the Satellites of the Planets and Pluto

TABLE II References for the composite spectra of Europa, Ganymede, and Callisto, from Calvin et al. 1995.

7. References

Bell, J. F., Clark, R. N., McCord, T. B. and Cruikshank, D. P. (1979). Reflection spectra of Pluto and three distant satellites, Bull. Amer. Astron. Soc., 11, 570 (abstract).

Bell, J. F., Cruikshank, D. P. and Gaffey, M. J. (1985) The composition and origin of the Iapetus dark material, Icarus, 61, 192-207.

Brown, R. H. (1982) The satellites of Uranus: Spectrophotometric and radiometric studies of their surface properties and diameters. Ph.D. thesis, Univ. of Hawaii, 158 pp.

Brown, R. H. (1983) The Uranian satellites and Hyperion: New spectrophotometry and compositional implications, Icarus, 56, 414-425.

Brown, R. H. and Clark, R. N. (1984) Surface of Miranda: Identification of water ice. Icarus, 58, 288-292.

Brown, R. H. and Cruikshank, D. P. (1983) The Uranian satellites: Surface compositions and opposition brightness surges, Icarus, 55, 83-92.

Brown, R. H., Cruikshank, D. P. and Morrison, D. (1982) Diameters and albedos of satellites of Uranus, Nature, 300, 423-425.

Brown, R. H., Cruikshank, D. P., Tokunaga, A. T., Smith, R. G. and Clark, R. N. (1988) Search for volatiles on icy satellites, Icarus, 74, 262-271.

Buratti, B. J. (1991) Ganymede and Callisto: Surface textural dichotomies and photometric analysis, Icarus, 92, 312-323.

Buratti, B. J., Mosher, J. A. and Johnson, T. V. (1990a) Albedo and color maps of the Saturnian satellites, Icarus, 87, 339-357.

Buratti, B. J., Wong, F. and Mosher, J. (1990b) Surface properties and photometry of the Uranian satellites, Icarus, 84, 203-214.

Buratti, B. J. and Mosher. J. A. (1995) The dark side of Iapetus: Additional evidence for an exogenous origin, Icarus, 115, 219-227.

Calvin, W. M. and Clark, R. N. (1991) Modeling the reflectance spectrum of Callisto 0.25-4.1 μm, Icarus, 89, 305-317.

Calvin, W. M. and Clark, R. N. (1993) Spectral distinctions between the leading ahd trailing hemispheres of Callisto: New observations, Icarus, 104, 69-78.

Calvin, W. M. and Spencer, J. R. (1994) Identification of O_2 on Ganymede. Bull. Am. Astron. Soc., 26. 1159 (abstract).

Calvin, W. M., Clark, R. N., Brown, R. H. and Spencer, J. R. (1995a) Spectra of the icy Galilean satellites from 0.2 to 5 μm: A compilation, new observations and a recent summary, J. Geophys. Res.-Planets, 1995 (in press).

Calvin, W. M., Spencer, J. R. and Johnson, R. E. (1995b) Formation of O_2 on Ganymede, Science (submitted), 1995.

Clark, R. N. and Lucey, P. G. (1984) Spectral properties of ice-particulate mixtures and implications for remote sensing. 1. Intimate mixtures. J. Geophys. Res, 89, 6341-6348.

Clark, R. N. and Roush, T. L. (1984) Reflectance spectroscopy: Quantitative analysis techniques for remote sensing applications, J. Geophys. Res., 89, 6329-6340.

Clark, R. N., Brown, R. H., Nelson, M. L. and Hayashi, J. (1983), Surface composition of Enceladus. Bull. Amer. Astron. Soc., 15, 853 (abstract).

Clark, R. N., Brown, R. H., Owensby, P. D. and Steele, A. (1984) Saturn's satellites: Near-infrared spectrophotometry (0.65-2.5 μm) of the leading and trailing sides and compositional implications, Icarus, 58, 265-281.

Clark, R. N., Fanale, F. P., and Gaffey, M. J. (1986) Surface composition of satellites. In Burns, J. and Matthews, M. S. (eds), Satellites, Univ. of Arizona Press, Tucson, 437-491.

Clark, R. N., Singer, R. B., Owensby, P. D. and Fanale, F. P. (1980) Galilean satellites: High precision near-infrared spectrophotometry (0.625-2.5 μm) of the leading and trailing sides, Bull. Am. Astron. Soc., 12, 713-714 (abstract).

Cruikshank, D. P. (1980) Near-infrared studies of the satellites of Saturn and Uranus, Icarus, 41, 246-258.

Cruikshank, D. P. and Brown, R. H. (1981) The Uranian satellites: Water ice on Ariel and Umbriel, Icarus, 45, 607-611.

Cruikshank, D. P. and Brown, R. H. (1986) Satellites of Uranus and Neptune, and the Pluto-Charon system. In Burns, J. and Matthews, M. S. (eds) Planetary Satellites, Univ. of Arizona Press, 836-873.

Cruikshank, D. P., Veverka, J. and Lebofsky, L. A. (1984) Satellites of Saturn: Optical properties. In Gehrels, T. and Matthews, M. S. (eds), Saturn, Univ. Arizona Press, Tucson, 640-667.

Cruikshank, D. P. Roush, T. L., Owen, T. C., Geballe, T. R., de Bergh, C., Schmitt, B., Brown, R. H. and Bartholomew, M. J.

(1993) Ices on the surface of Triton, Science, 261, 742-745.

Cruikshank, D. P., Roush, T. L., Owen, T. C., Quirico, E. and DeBergh, C. (1996) The surface compositions of Triton, Pluto, and Charon. In [this volume].

Domingue, D. L., Hapke, B. W., Lockwood, G. W. and Thompson, D. T. (1991) Europa's phase curve: Implications for surface structure, Icarus, 90, 30-42.

Domingue, D. L., Lane, A. L., Price, S. K. and Lankton, M. (1994) Have the UV reflectance spectra of the Galilean satellites Io and Europa changed with time? Bull. Am. Astron. Soc., 26, 1158-1159 (abstract).

Griffith, C. Moeckel, R., Cruikshank, D., Pendleton, Y., Brown, R. H., Owen, T., Geballe, T. and Joyce, D. (1995) Near-ir spectra of the surfaces of Titan, Rhea, Iapetus, and Enceladus. Paper presented at conference on Solar System Ices, Toulouse 27-30 March.

Hapke, B. W. (1993a) Combined theory of reflectance and emittance spectroscopy. In Pieters, C. M. and Englert, P. A. J. (eds.) Remote Geochemical Analysis: Elemental and Mineralogical Composition. Cambridge Univ. Press, New York, pp 31-42.

Hapke, B. W. (1993b) Reflectance and Emittance Spectroscopy. Cambridge Univ. Press, New York, 455 pp.

Hillier, J., Helfenstein, P., and Veverka, J. Miranda (1989) Color and albedo variations from Voyager photometry, Icarus, 82, 314-335.

Kuiper, G. P. (1957) Infrared observations of planets and satellites. Astron. J., 62, 295 (abstract).

Lane, A. L., Nelson, R. M. and Matson, D. L. (1981) Evidence for sulphur implantation in Europa's UV absorption band, Nature, 292, 38-39.

Lane, A. L., Domingue, D. L., Price, S. K. and Lankton, M. (1994) A re-examination of IUE near-UV data: Have Ganymede and Callisto changed with time? Bull. Am. Astron. Soc., 26, 1159 (abstract).

Lanzerotti, L. J., Brown, W. L., Maclennan, C. G., Cheng, A. F., Krimigis, S. M. and Johnson, R. E. (1987) Effects of charged particles on the surfaces of the satellites of Uranus, J. Geophys. Res., 92, 14,949-14,957.

Lebofsky, L. A. and Feierberg, M. A. (1985) 2.7-4.1-μm spectrophotometry of icy satellites of Saturn and Jupiter, Icarus, 63, 237-242.

McFadden, L. A., Bell, J. F. and McCord, T. B. (1980) Visible spectral reflectance measurements (0.33-1.1 μm) of the galilean

satellites at many orbital phase angles, Icarus, 44, 410-430.

Morrison, D., Johnson, T. V., Shoemaker, E. M., Soderblom, L. A., Thomas, P., Veverka, J. and Smith, B. A. (1984) Satellites of Saturn: Geological perspective. In Gehrels, T. and Matthews, M. W. (eds), Univ. Arizona Press, Tucson, 609-639.

Morrison, D., Owen, T., and Soderblom, L. A. (1986) The satellites of Saturn. In Burns, J. and Matthews, M. W. (eds), Univ. Arizona Press, Tucson, 764-801.

Nelson, R. M., Lane, A. L., Matson, D. L., Veeder, G. J., Buratti, B. J. and Tedesco, E. F. (1987a) Spectral geometric albedos of the Galilean satellites from 0.24 to 0.34 micrometers: Observations with the International Ultraviolet Explorer, Icarus, 72, 358-380.

Nelson, R. M., Buratti, B. J., Wallis, B. D., Lane, A. L., West, R. A., Simmons, K. E., Hord, C. W. and Esposito, L. W. (1987b) Voyager 2 photopolarimeter observations of the Uranian satellites, J. Geophys. Res., 92, 14,905-14,910.

Noll, K. S. and Knacke, R. F. (1993) Titan: 1-5 μm photometry and spectrophotometry and a search for variability, Icarus, 101, 272-281.

Noll, K. S., Weaver, H. A., and Gonnella, A. M. (1995) The albedo spectrum of Europa from 2200 A to 3300 A, J. Geophys. Res. Planets (in press).

Ockert, M. E., Nelson, R. M., Lane, A. L. and Matson, D. L. (1987) Europa's ultraviolet abosorption band (260-320 nm): Temporal and spatial evidence from IUE, Icarus, 70, 499-505.

Owen, T. C., Roush, T. L., Cruikshank, D. P., Elliot, J. L., Young, L. A., de Bergh, C., Schmitt, B. Geballe, T. R., Brown, R. H. and Bartholomew, M. J. (1993) Surface ices and the atmospheric composition of Pluto, Science, 261, 745-748.

Pollack, J. B., Witteborn, F. C., Erickson, E. F., Strecker, D. W., Baldwin, B. J. and Bunch, T. E. (1978) Near-infrared spectra of the galilean satellites: Observations and compositional implications, Icarus, 36, 271-303.

Roush, T. L. (1994) Charon: More than water ice? Icarus, 108, 243-254

Roush, T. L., Pollack, J. B., Witteborn, F. C., Bregman, J. D., and Simpson, J. P. (1990) Ice and minerals on Callisto: A reassessment of the reflectance spectra, Icarus, 86, 355-382.

Roush, T. L., Cruikshank, D. P., and Owen, T. C. (1995) Surface ices in the outer solar system. In Farley, K. A. (ed), Volatiles in the Earth and Solar System,. Am. Inst. Physics, NY.

Sack, N. J., Johnson, R. E., Boring, J. W. and Baragiola, R. A. (1992) The effect of magnetospheric ion bombardment on the reflectance of Europa's surface, Icarus, 100, 534-540.

Schmitt, B., de Bergh, C., Lellouch, E., Maillard, J-P., Barbe, A. and Douté, S. (1994) Identification of three absorption bands in the 2-μm spectrum of Io, Icarus, 111, 79-105.

Sill, G. T. and Clark, R. N. (1982) Compositions of the surfaces of the Galilean satellites. In Morrison, D. (ed), Satellites of Jupiter, Univ. of Arizona Press, Tucson, 174-212.

Soifer, B. T., Neugebauer, G. and Matthews, K. (1981) Near-infrared spectrophotometry of the satellites and rings of Uranus, Icarus, 45, 612-617.

Spencer, J. R., Calvin, W. M. and Person, M. J. (1995) CCD spectra of the Galilean satellites: Molecular oxygen on Ganymede, J. Geophys. Res. Planets (in press).

Stevenson, D. (1982) Volcanism and igneous processes in small icy satellites, Nature, 298, 142-144.

Thomas, P. and Veverka, J. (1985) Hyperion: Analysis of Voyager observations, Icarus, 64, 414-424.

Thomas, P., Veverka, J. and Dermott, S. (1986) Small satellites. In Satellites, Burns, J. and Matthews, M. S. (eds), Univ. Arizona Press, Tucson, 802-835.

Thompson, W. R., Murray, B. G. J. P. T., Khare, B. N. and Sagan, C. (1987) Coloration and darkening of methane clathrate and other ices by charged paticle irradiation: Application to the outer solar system, J. Geophys. Res., 92, 14,933-14,947.

Verbicer, A. J. and Helfenstein, P. (1995) Reflectance spectroscopy of icy surfaces. Paper presented at Solar System Ices conference, Toulouse, 27-30 March.

Verbicer, A. J. and Veverka, J. (1989) Albedo dichotomy of Rhea: Hapke analysis of Voyager photometry, Icarus, 82, 336-353.

Veverka, J., Thomas, P., Helfenstein, P., Brown, R. H. and Johnson, T. V. (1987) Satellites of Uranus: Disk-integrated photometry from Voyager imaging observations, J. Geophys. Res., 92, 14,895-14,904.

Veverka, J., Brown, R. H. and Bell, J. F. (1991) Uranus satellites: Surface properties. In Bergstralh, J. T., Miner, E. D., and Matthews, M. S. (eds), Uranus, Univ. of Arizona Press, Tucson, 528-560.

Warren, S. G. (1984) Optical constants of ice from the ultraviolet to the microwave, Appl. Opt., 23, 1206-1225.

Wilson, P. D., Sagan, C. and Thompson, W. R. (1994) The organic surface of 5145 Pholus: Constraints set by scattering theory, Icarus, 107, 288-303.

Wilson, P. D. and Sagan, C. (1995) Spectrophotometry and organic matter on Iapetus, I, Compositional models, J. Geophys. Res. 100, 7531-7537.

Figure 1. Grain-size effects in H_2O ice. These synthetic spectra of H_2O ice were calculated by Hapke theory from optical constants for ice near the freezing point from Warren (1984).

Figure 2. Reflectance spectra of the leading and trailing hemispheres of Europa from the compilation by Calvin et al. (1995a). References to the sources of various components of the composite are found in Table II.

Figure 3. Reflectance spectrum of Europa's leading hemisphere from Calvin et al. (1995a), with a synthetic spectrum of H_2O ice (100 μm grains) calculated from the optical constants of Warren (1984). References to the sources of various components of the composite are found in Table II.

Figure 4. Reflectance spectra of the leading and trailing hemispheres of Ganymede from Calvin et al. (1995a). References to the sources of various components of the composite are found in Table II.

Figure 5. Reflectance spectra of the leading and trailing hemispheres of Callisto from Calvin et al. (1995a). References to the sources of various components of the composite are found in Table II.

Figure 6. Reflectance spectra of the leading and trailing hemispheres of Callisto, with models calculated from the optical constants of H_2O ice, serpentine, and magnetite (Roush et al. 1990).

Figure 7. Reflectance spectra of the satellites of Saturn, using data (0.65-2.5 μm) from Clark et al. (1984) scaled to the Voyager photometric results derived by Buratti et al. 1990a)

Figure 8. Reflectance spectra of the satellites of Uranus from various sources. The portions of the spectra between 0.8 and 2.5 μm come from Brown (1983) and Brown and Cruikshank (1983). For Titania and Oberon, the portions from 0.32-0.9 come from Bell et al. (1979), first published in Brown (1983). The open triangles represent the five filter observations of the Imaging Science System and two wavelengths from the Photopolarimeter System on Voyager 2 (Buratti et al. 1990b). The adjustment of the longer wavelength data to geometric albedo for Titania and Oberon was accomplished by scaling to the Voyager data in the region of spectral overlap. The spectra of Ariel and Umbriel were scaled to geometric albedo using JHK photometry of these satellites and Titania and Oberon (Cruikshank 1980) plus values of the V magnitudes from the **Astronomical Almanac** for 1995. The long wavelength data for Miranda are from Brown and Clark (1984) and are normalized to 1.0 at the peak of the spectrum. The discontinuity in the spectral geometric albedo for Ariel may arise from phase angle effects and warrants further study.

Figure 9. The reflectance spectra of three H_2O-bearing satellites of three different planets are shown here for comparison. Values of the single-scattering albedos from the work of Verbiscer and Helfenstein; (1995) are shown. This figure illustrates the great differences among ice-bearing satellites; although all three have surfaces dominated by H_2O ice, their reflectances are quite dissimilar.

TABLE I

The Ice-Covered Satellites of the Planets

Planet	Satellite	Radius km	Ices (Molecules) Detected
Jupiter	Io	1815	SO_2, H_2S (?), H_2O (?)
	Europa	1569	H_2O, SO_2
	Ganymede	2631	H_2O, O_2
	Callisto	2400	H_2O
Saturn	Mimas	195	H_2O?
	Enceladus	250	H_2O
	Tethys	530	H_2O
	Dione	560	H_2O
	Rhea	765	H_2O
	Hyperion	irr*	H_2O
	Iapetus	730	H_2O
	[Rings]	-	H_2O
Uranus	Miranda	240	H_2O
	Ariel	579	H_2O
	Umbriel	586	H_2O
	Titania	790	H_2O
	Oberon	762	H_2O
Neptune	Triton	1360	N_2, CH_4, CO, CO_2
Pluto	[itself]	1190	N_2, CH_4, CO
	Charon	600	H_2O

* The shape of Hyperion is irregular; its roughly triaxial dimensions (radii) are 205 X 130 X 110 km.

Table II

References for the composite spectra of Europa, Ganymede, and Callisto, from Calvin et al. 1995.

Europa

Wavelength Region (μm)	Leading Hemisphere	Trailing Hemisphere
0.24-0.34	Nelson et al. 1987	same
0.4-1.1	Spencer et al. 1995	McFadden et al. 1980
0.8-2.0	Brown et al. 1988	Clark et al. 1986
2.0-2.5	Calvin et al. 1995	same
2.2-4.2	Lebofsky and Feierberg 1985	same
4.6-5.0	Noll and Knacke 1993	--

Ganymede

Wavelength Region (μm)	Leading Hemisphere	Trailing Hemisphere
0.24-0.34	Nelson et al. 1987	same
0.4-1.1	McFadden et al. 1980	Spencer et al. 1995
0.8-2.5	Clark et al. 1986	Clark et al. 1980
2.4-4.2	Pollack et al. 1978	--
2.8-3.9	--	Calvin et al. 1995
4.5-5.2	Noll and Knacke 1993	--

Callisto

Wavelength Region (μm)	Leading Hemisphere	Trailing Hemisphere
0.24-0.34	Nelson et al. 1987	same
0.4-1.1	Spencer et al. 1995	McFadden et al. 1980
0.8-1.9	Calvin and Clark 1991, 1993	Calvin and Clark 1991
1.9-4.2	Calvin and Clark 1993	same
4.6-5.2	Noll and Knacke 1993	Roush et al. 1990

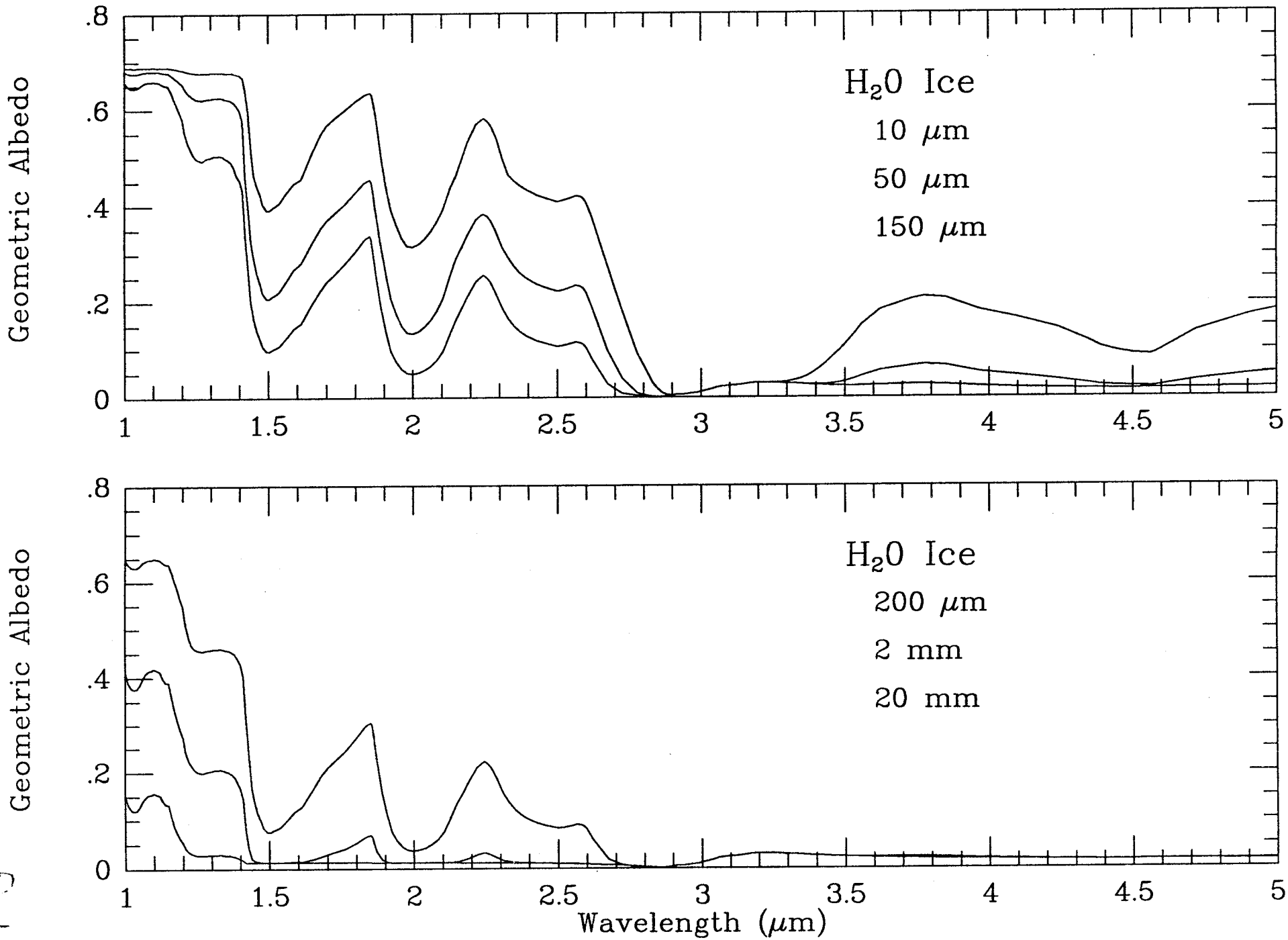

based on Warren, 1984

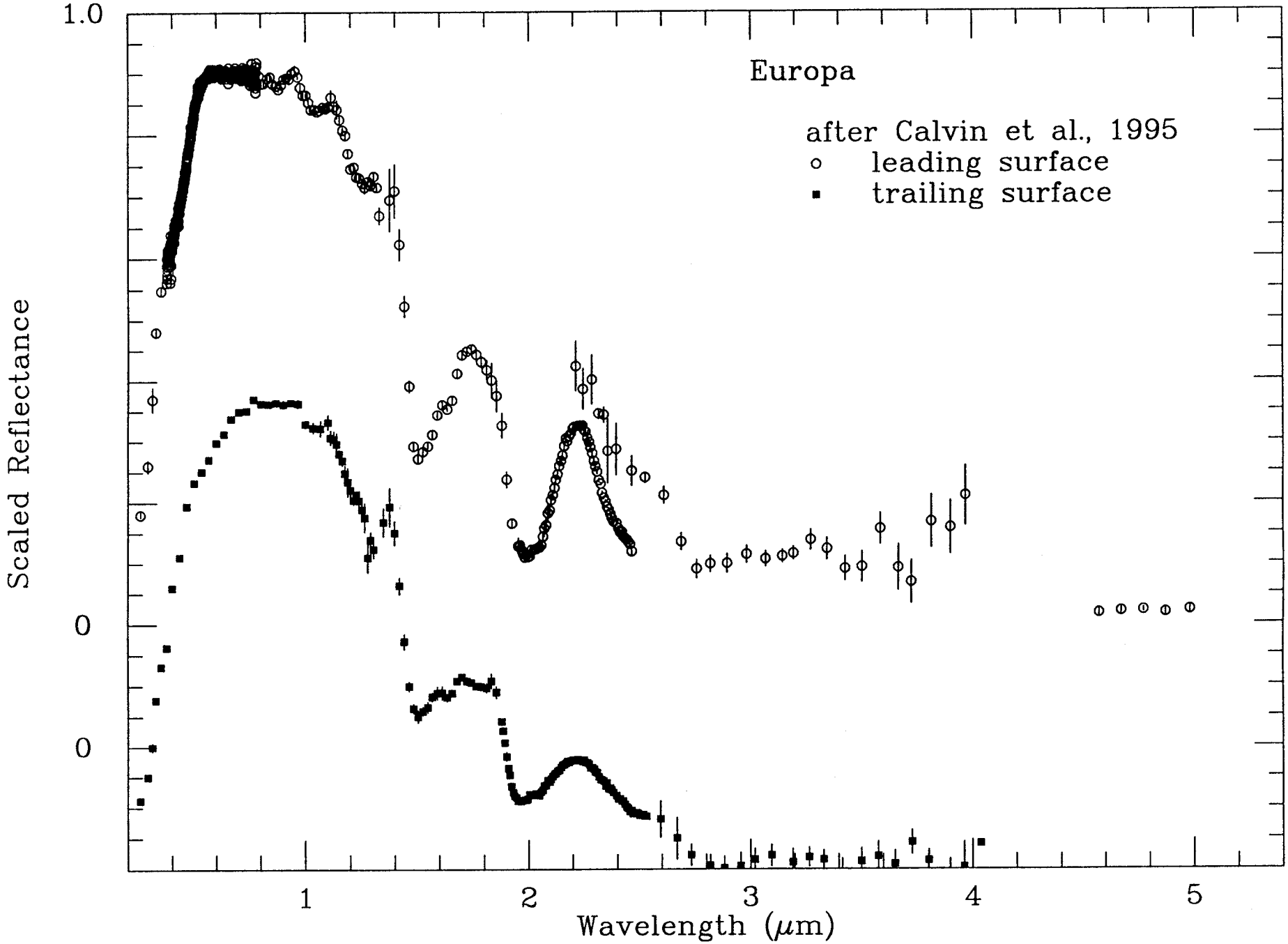
Europa
after Calvin et al., 1995
leading surface
trailing surface
Scaled Reflectance
1.0
0
0
1
2
3
4
5
Wavelength (μm)

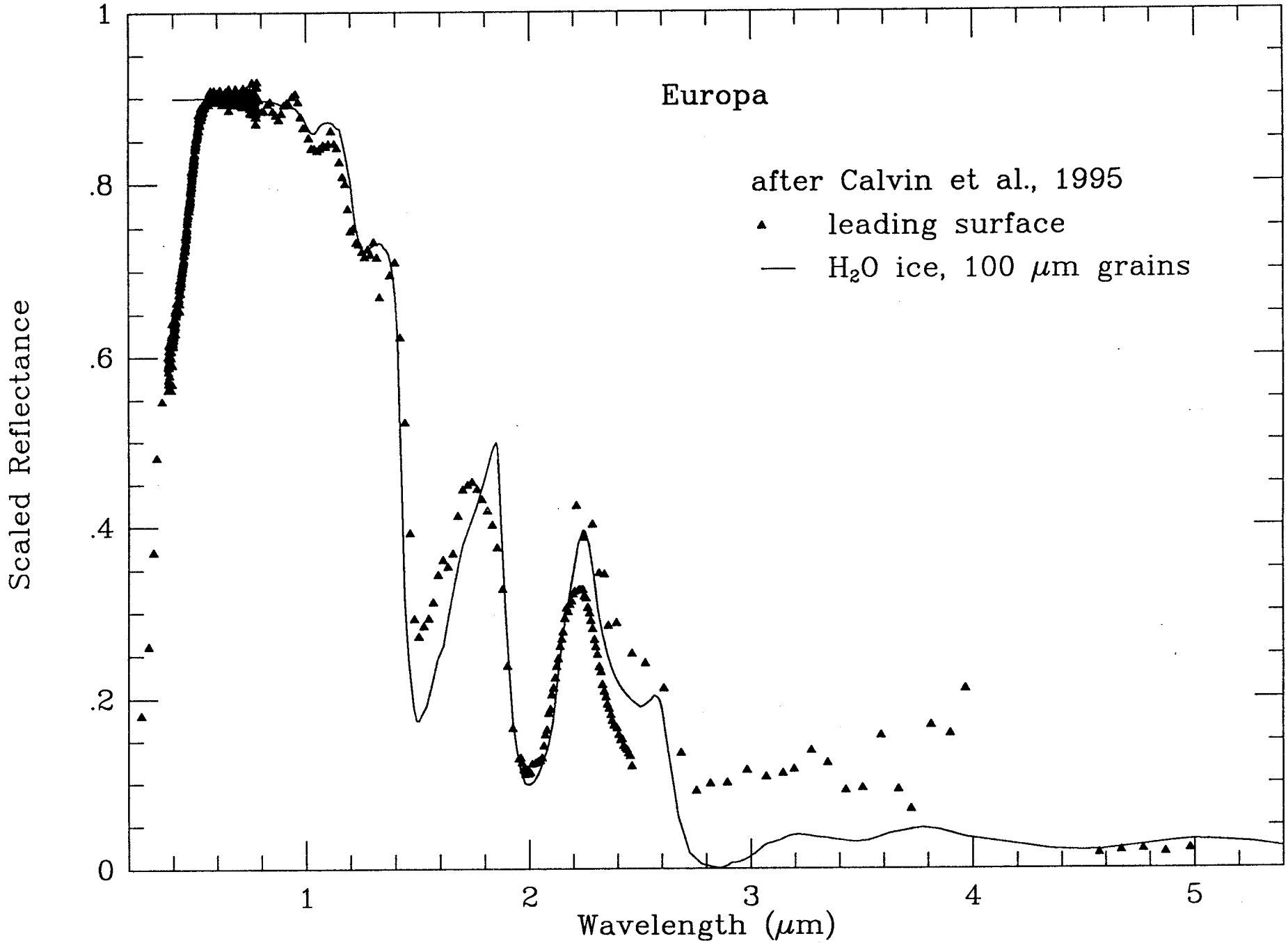
Europa
after Calvin et al., 1995
leading surface
H_2O ice, 100 μm grains
Scaled Reflectance
Wavelength (μm)
0
.2
.4
.6
.8
1
1
2
3
4
5

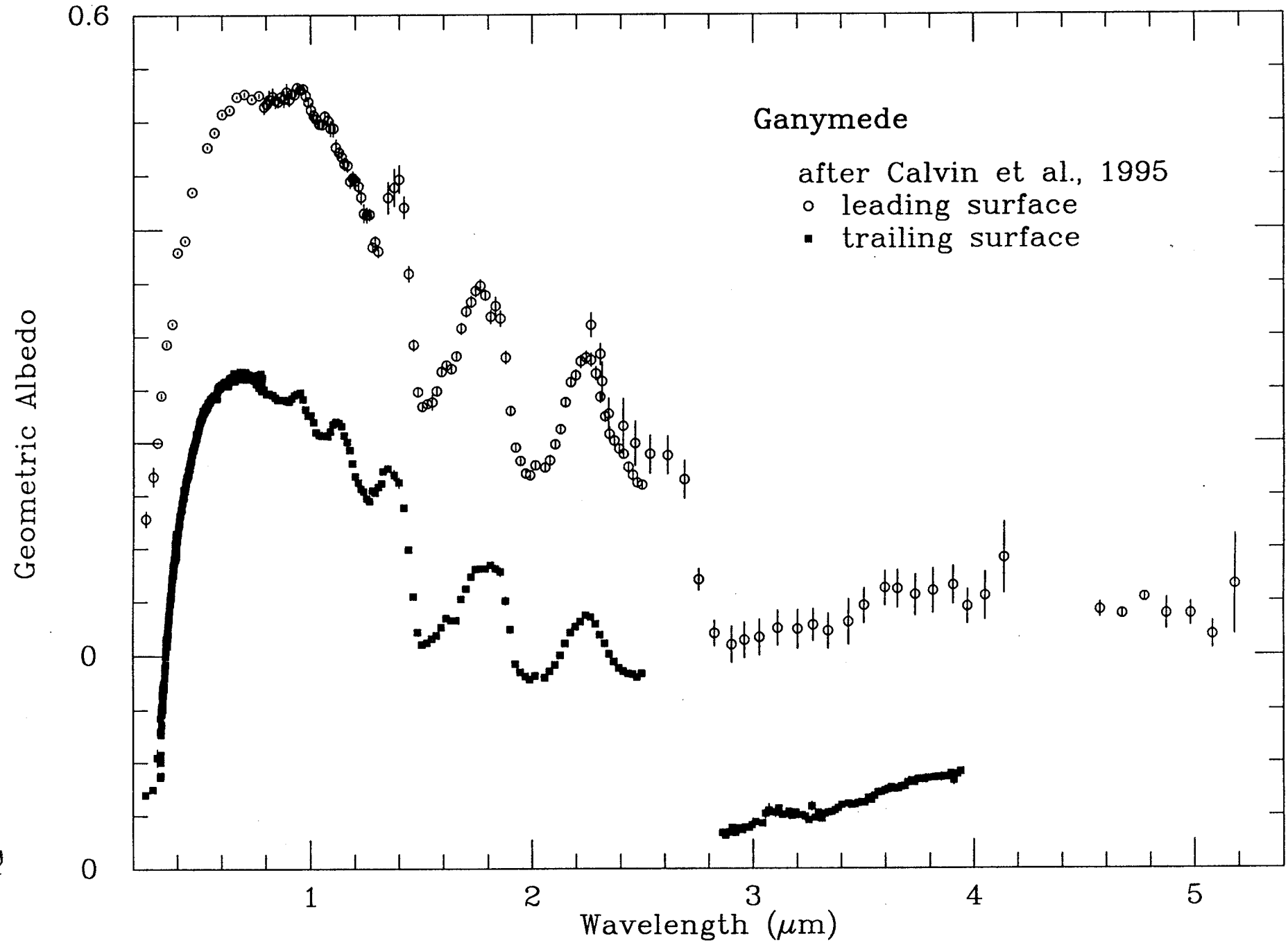
Ganymede
after Calvin et al., 1995
leading surface
trailing surface
Geometric Albedo
0.6
0
0
1
2
3
4
5
Wavelength (μm)

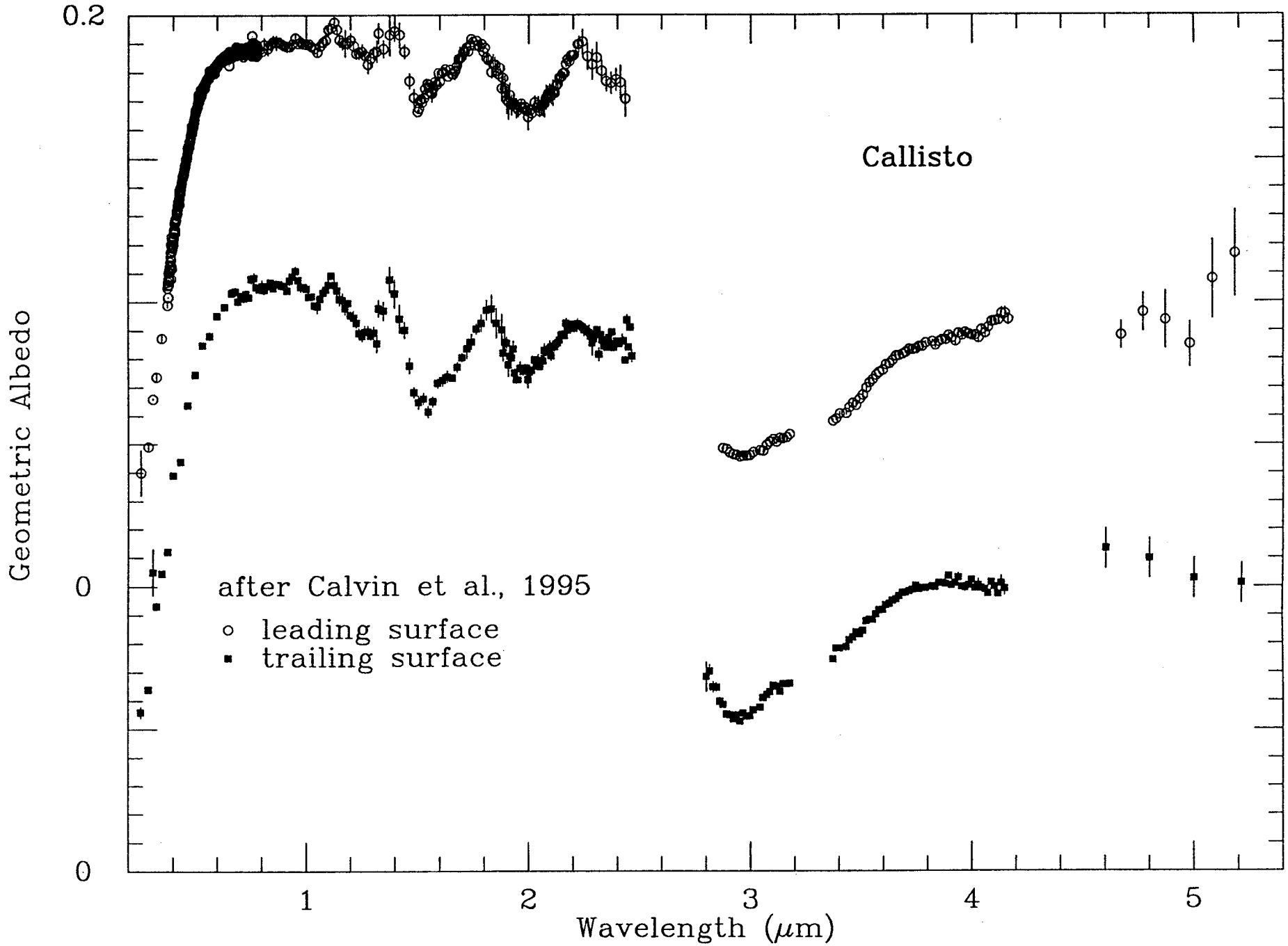
0.2
0
0
Geometric Albedo
Callisto
after Calvin et al., 1995
leading surface
trailing surface
1
2
3
4
5
Wavelength (μm)

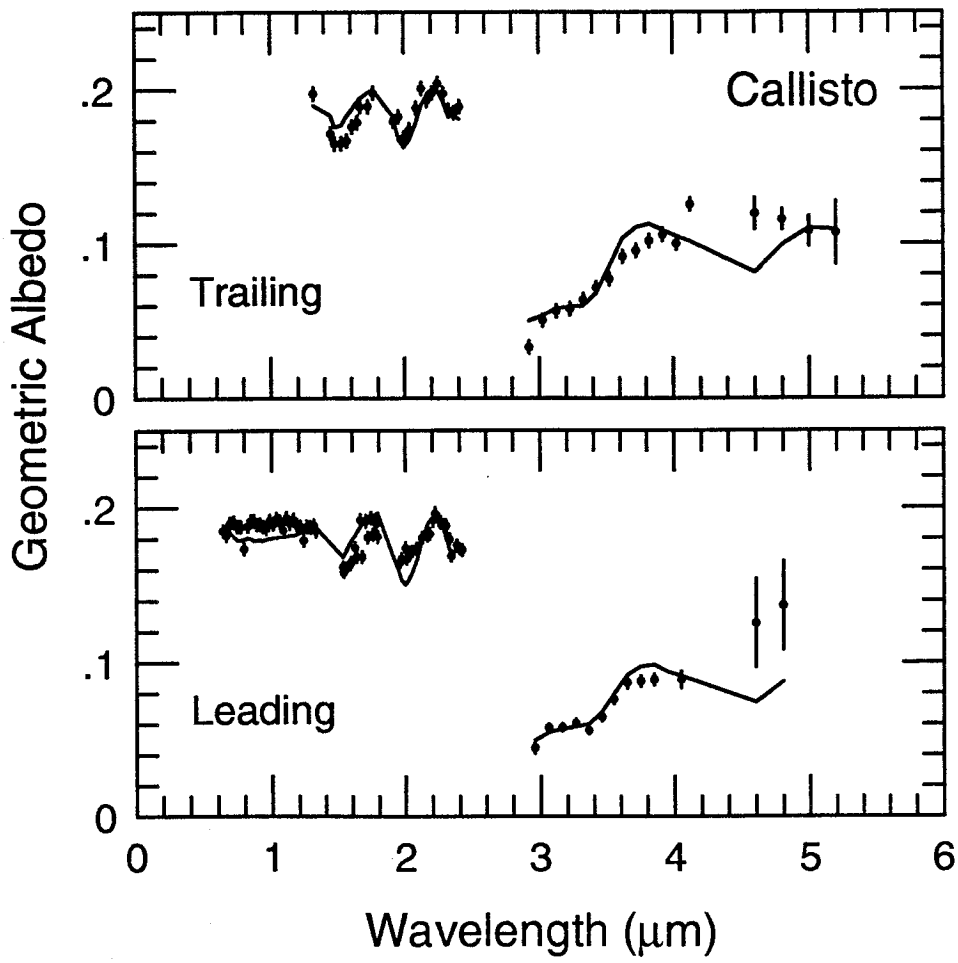
Callisto
Trailing
Leading
Geometric Albedo
.2
.1
0
0
1
2
3
4
5
6
Wavelength (μm)

Figure 6

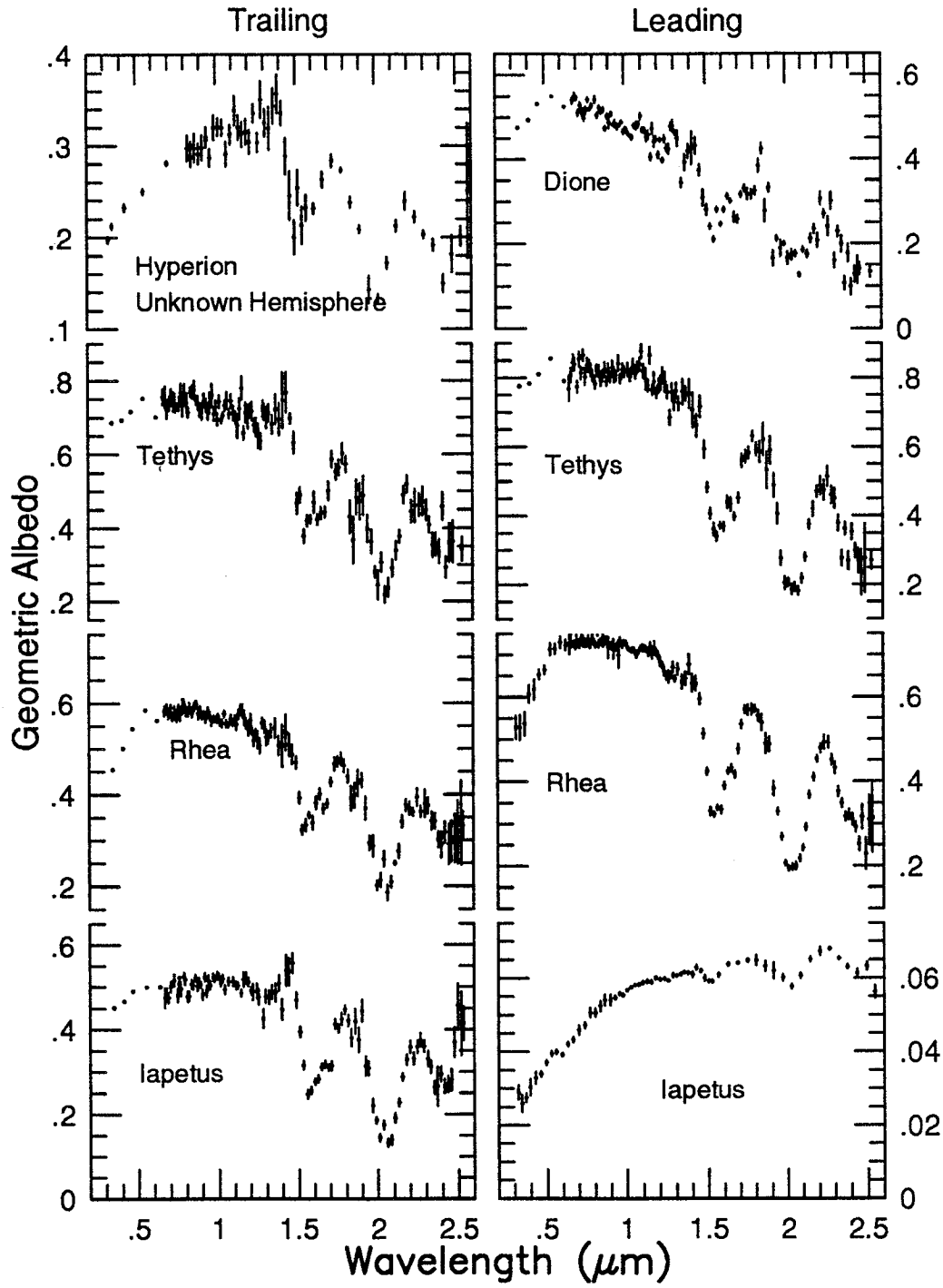
Trailing
Leading
Hyperion
Unknown Hemisphere
Dione
Tethys
Tethys
Rhea
Rhea
Iapetus
Iapetus
Geometric Albedo
Wavelength (μm)
.4
.3
.2
.1
.6
.4
.2
0
.8
.6
.4
.2
.6
.4
.2
.6
.4
.2
.06
.04
.02
0
.5
1
1.5
2
2.5

Figure 7

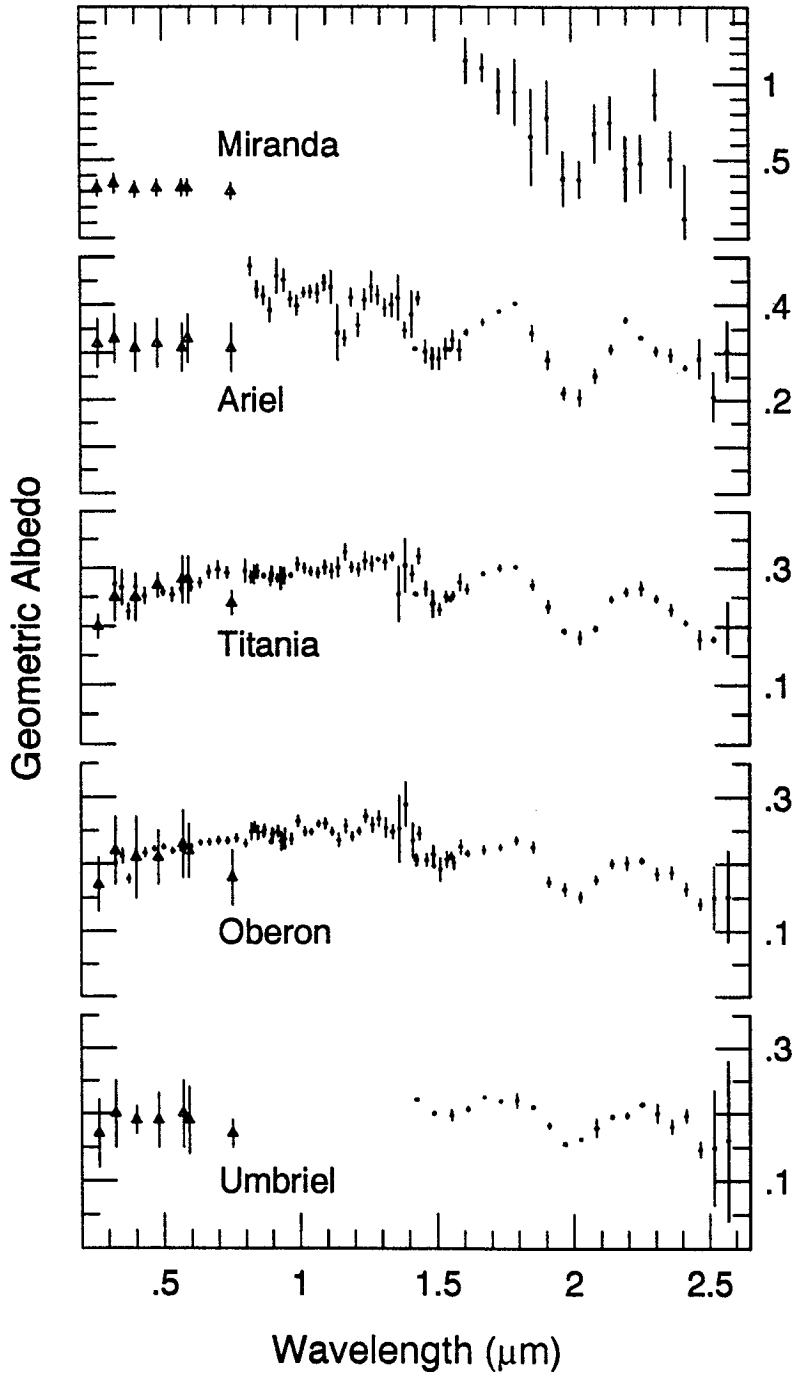
Miranda
Ariel
Titania
Oberon
Umbriel
Geometric Albedo
Wavelength (μm)
1
.5
.4
.2
.3
.1
.3
.1
.3
.1
.5
1
1.5
2
2.5

Figure 8

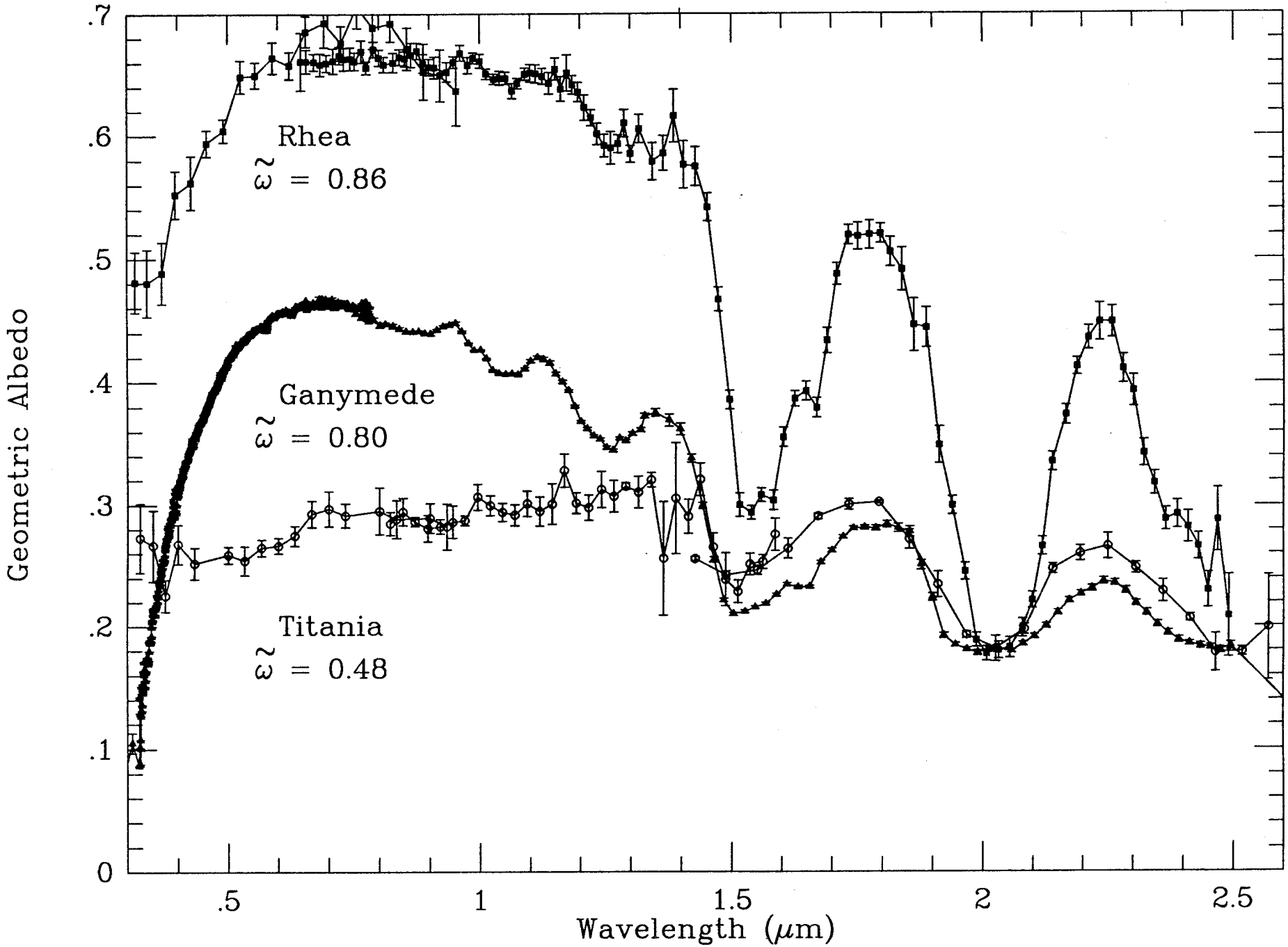
Geometric Albedo
Wavelength (μm)
Rhea
ω̃ = 0.86
Ganymede
ω̃ = 0.80
Titania
ω̃ = 0.48
0
.1
.2
.3
.4
.5
.6
.7
.5
1
1.5
2
2.5

Figure 9